Robotica (2010) volume 28, pp. 637–648. © Cambridge University Press 2009
doi:10.1017/S0263574709990294

A biologically inspired method for robot navigation in a cluttered environment

Hamid Teimoori* and Andrey V. Savkin

School of Electrical Engineering and Telecommunications, The University of New South Wales, Sydney, Australia

(Received in Final Form: June 24, 2009. First published online: August 11, 2009)

SUMMARY

The problem of wheeled mobile robot (WMR) navigation toward an unknown target in a cluttered environment has been considered. The biologically inspired navigation algorithm is the equiangular navigation guidance (ENG) law combined with a local obstacle avoidance technique. The collision avoidance technique uses a system of active sensors which provides the necessary information about obstacles in the vicinity of the robot. In order for the robot to avoid collision and bypass the enroute obstacles, the angle between the instantaneous moving direction of the robot and a reference point on the surface of the obstacle is kept constant. The performance of the navigation strategy is confirmed with computer simulations and experiments with ActivMedia Pioneer 3-DX wheeled robot.

KEYWORDS: Wheeled robot; Biologically inspired navigation; Obstacle avoidance.

1. Introduction

The research on wheeled mobile robot navigation with obstacle avoidance has gained a great deal of interest over the past few years. Mobile robots have been used to solve different encountered problems and replace, augment or support human activities in several indoor or outdoor applications, such as factory and mining automation,[40] home and office assistance,[14] interactive guide system in museums,[16] search and rescue operations,[48] exploration in hazardous environments,[20] and military systems[47]. In all of these applications since the safety of the mobile robot and the people around are of prime importance, the robot should be equipped with a navigation system which combines a guidance strategy that guides the robot toward a target, with a collision avoidance technique, which leads the robot safely around an obstacle.

Many sophisticated approaches in guidance and control of a wheeled robot for target following and trajectory tracking have been proposed in the literature, including: nonlinear control,[17,39] dynamic feedback linearizing,[10] sliding mode control,[49] fuzzy control,[35] and neural network.[20] A real-time target tracking control scheme based on fuzzy sliding-mode control strategy was suggested in ref. [26]. A strategy in robot navigation based on proportional navigation guidance was proposed in refs. [2, 28] introduced a precision guidance law with impact angle constraint for a 2D planar intercept.

However, in most of the current methods, target velocity, position, moving direction or line-of-sight (LOS) angle (the angle between the reference line and the imaginary straight line starts at the robot's reference point and is directed toward the target's position) are considered given, which are not always available in practice. Global positioning system (GPS) can provide accurate location information in outdoor settings; however, they fail in indoor navigation where GPS signals cannot be reliably received. Video or infrared (IR) based positioning systems, similarly, are restricted to line-of-sight limitations or poor performance with fluorescent lighting, direct sunlight, and lack of light situations. Furthermore, in some applications the target is either too small to appear in an image frame or located behind an obstacle in indoor applications or too far from the robot in outdoor applications.

In order to safely navigate and reliably operate in populated environments, on the other side, an autonomous vehicle should be able to detect and avoid the obstacles on the way toward the target. Current motion planning and obstacle avoidance strategies can be classified according to different aspects: *local* (when the environment is completely or partially unknown) or *global* (when it is totally known); *online* (in which the path is generated incrementally) or *off-line* (when the entire path is computed before the robot makes its first move); *static* (when all the obstacles in the environment are stationary) or *dynamic* (with moving and stationary obstacles); and *reactive* (in which the most recent sensory perceptions are used to guide the robot toward the goal) or *map-based* (the robot is navigated based on a given map of the environment). A comprehensive summary of the available algorithms for motion planning and their classifications can be found in ref. [15].

Global sensor-based planners use the priory and sensory information to build a complete model of the environment and then try to find the best possible solution.[3,46]

While these approaches guarantee the global convergence to the target, their application is not always possible in practice, since on the first hand they need a complete information on exact target and obstacles positions and on the other hand they are highly computationally expensive. To generate a trajectory, local path planners use onboard sensors to locally observe a small fraction of an unknown environment at each time and as a results fail to generate optimal trajectories.[11,22] The short calculation time, in

* Corresponding author. E-mail: h.teimoori@unsw.edu.au

these strategies, allows the robot to react in real-time in confrontation with an enroute obstruction. Another example for local path planners, which is similar in flavor to ours, is the Bug family algorithms which are inspired by bugs behavior on crawling along a wall. Applying the Bug algorithm,[29] the robot directly travels toward the target and bypasses the enroute obstacles by following their boundaries in close range. Resuming motion toward the target happens only when a leaving condition, which monitors a globally convergent criterion, holds (see e.g., refs. [9, 29, 30] for further information on Bug1 and Bug2 algorithms and refs. [18, 19] for Tangent Bug and DistBug algorithms which are extensions of Bug2 algorithm). Another similar approach based on the visual information was also presented in ref. [13]. In spite of their simplicity, these strategies are all heuristic and kinematic equations of wheeled robots and their nonholonomic constraints, are not considered in these algorithms, which is a severe limitation.

In this paper, a new approach is proposed for the robot navigation toward an unknown target which combines a goal-directed navigation strategy, which ensures the global convergence to the target, with a local obstacle avoidance technique, which minimizes the computational burden on the planner. In this regards, considering dynamic constraints of the mobile robot, i.e., bounded linear and angular velocities, the equiangular navigation guidance (ENG) law which was initially proposed in ref. [41] is applied for the problem of robot navigation toward an unknown target using just the relative distance between the robot and target also known as LOS range. The LOS range can be estimated by measuring the strength of the signal transmitted by the target and received at the robot position.[41] Having applied the ENG law in an obstacle-free environment, the robot approaches the unknown target in a semi-equiangular spiral whose arc length and curvature are subjects to change with a control parameter.

However, to prevent from any collision with enroute obstacles, ENG is then combined with a low level obstacle avoidance strategy. This strategy uses a system of active sensors which provides the necessary information about the obstacles in the vicinity of the robot. In order for the robot to avoid collision and bypass the enroute obstacles, the angle between the instantaneous moving direction of the robot and a reference point on the surface of the obstacle is kept constant. Having applied the proposed avoidance strategy, the robot bypasses any obstruction on the way toward the target preserving a safety distance from the obstacle.

Researchers in the area of robot navigation are finding much inspiration from biology, where the problem of controlled animal motion is a central one.[25,34,50] Animals, such as insects, birds, or mammals, are believed to use simple, local motion control rules that result in remarkable and complex intelligent behaviors. The navigation approach toward a target, i.e., the ENG law, and the idea of local obstacle avoidance strategy which is proposed in this paper, are also inspired by biological examples such as an insect flying toward a candle and a squirrel running around a tree.[23,42] It has been observed that peregrine falcons which are among the fastest birds on the earth, plummet toward their targets at speeds of up to two hundred miles an hour along an equiangular spiral.[43] Inspired by landing strategies of honeybees, the strategy of moving along an spiral trajectory has been used in landing for light airplanes or unmanned aerial vehicles (UAVs).[8,37] Moreover, guidance strategies inspired by honeybee navigation were successfully applied in the problems of precision missile guidance,[31,32] and vision-based wheeled robot docking.[28]

The reminder of the paper is organized as follows. Problem description and model of the controlled wheeled robot and the target are introduced in Section 2. Section 3 presents an overview of the ENG law for approaching an unknown target and gives its mathematically rigorous analysis. Obstacle avoidance strategy has been proposed in Section 4. Section 5 denotes the overall navigation algorithm, which is derived from switching between the ENG law and the proposed local obstacle avoidance technique. Computer simulation results are given in Section 6. Section 7 describes experiments with ActivMedia Pioneer 3-DX wheeled robot. Finally, the paper is concluded in Section 8.

2. Problem Statement

Consider a three-wheeled, nonholonomic mobile robot of Dubin's car type, which moves in a horizontal plane and in an unknown environment. In a two-dimensional space, the position of the robot can be represented by a triplet $P_R = (X_R, Y_R, \theta_R)$ where (X_R, Y_R) is the location of the middle of the wheel base and θ_R is the heading angle with respect to the reference line. Let V_R be the linear velocity and ω_R the angular velocity of mobile robot. A rolling-without-slippage model is assumed for the robot. The motion model is classically given by

$$\begin{aligned} \dot{X}_R &= V_R \cos(\theta_R), \\ \dot{Y}_R &= V_R \sin(\theta_R), \\ \dot{\theta}_R &= \omega_R, \end{aligned} \tag{2.1}$$

with $U = [V_R \ \omega_R]^T$ as the control vector of the mobile robot, $U \in V \times [-\omega_{\max} \ \omega_{\max}]$ with $V > 0$ and $\omega_{\max} > 0$.

We consider the case of a stationary target, located at unknown position $P_T = (X_T, Y_T)$. The only available information from the target is the relative distance between the robot and target or the LOS range. The robot moves only in forward direction with constant linear velocity except in the vicinity of target.

Given the robot position and orientation with respect to the target position in the polar coordinate system, we define LOS range d and the angle between the front direction and the target direction, λ_R, as shown in Fig. 1:

$$\begin{aligned} d &= \sqrt{d_x^2 + d_y^2}, \\ \lambda_R &= \psi_R - \theta_R, \end{aligned} \tag{2.2}$$

where ψ_R is the LOS angle and $|\lambda_R| \leq \pi$. The robot-target motion is expressed by

$$\dot{d} = -V_R \cos(\lambda_R) \tag{2.3a}$$

$$\dot{\lambda}_R = -\omega_R + \frac{V_R}{d} \sin(\lambda_R). \tag{2.3b}$$

https://doi.org/10.1017/S0263574709990294

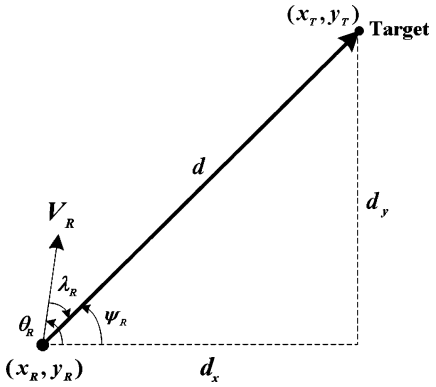

Fig. 1. Robot position and orientation with respect to target.

Note that the kinematic Eq. (2.3) are only valid for nonzero values of the LOS range, since λ_R is undefined for $d = 0$.

We also consider an unknown environment with static obstacles. Obstacles can be of any concave or convex shapes and their positions or geometrical distributions are unknown to the robot. It is assumed that the robot is equipped with a set of range sensors which provide range and angle to the enroute obstacles.

The objective is to design a collision-free navigation law, which allows the robot to approach a target using only measurements of the relative distance d between the robot and target and simultaneously avoid the obstacles on the way while keeping a safety distance from them.

3. Equiangular Navigation Guidance Law

We assume that the distance $d(t)$ to the target and its derivative $\dot{d}(t)$ are both available to the robot controller. Furthermore, it is assumed that the robot linear velocity is constant:

$$V_R(t) \equiv V_{R0} > 0. \tag{3.4}$$

In this case, the minimal turning radius of the robot is

$$R_{\min} = \frac{V_{R0}}{\omega_{\max}}. \tag{3.5}$$

We wish to introduce a robot navigation law of the form

$$\omega_R(t) = \mathcal{F}\left(d(\cdot)\,|_0^t, \dot{d}(\cdot)\,|_0^t\right). \tag{3.6}$$

Of course, the navigation law (3.6) must satisfy the constraint

$$-\omega_{\max} \le \omega_R(t) \le \omega_{\max}. \tag{3.7}$$

We will consider the case of a steady target

$$X_T(t) \equiv X_{T0}, \quad Y_T(t) \equiv Y_{T0}.$$

Definition 3.1. A navigation law of the form (3.6) is said to be encircling if it satisfies Eq. (3.7) and for any steady target location the robot guided by this law after a certain finite time moves along a circle of the minimal turning radius (3.5) such that the steady target lies inside this circle.

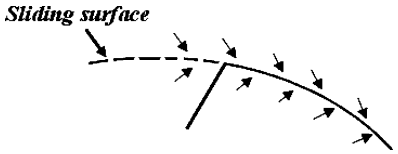

Fig. 2. An illustration of sliding surface in sliding mode control.

Suppose that the following assumption holds

$$d(0) > 4R_{\min}. \tag{3.8}$$

Let L be a given constant such that

$$0 < L < V_{R0}. \tag{3.9}$$

We introduce the following navigation law:

$$\omega_R(t) = \omega_{\max}\,\mathrm{sgn}(L + \dot{d}(t)). \tag{3.10}$$

where

$$\mathrm{sgn}(\alpha) := \begin{cases} 1 & if \ \alpha > 0 \\ 0 & if \ \alpha = 0 \\ -1 & if \ \alpha < 0. \end{cases} \tag{3.11}$$

We will need the following assumption:

$$\lambda_R(0) \neq -\arccos\left(\frac{L}{V_R}\right). \tag{3.12}$$

Now we are in a position to give a mathematical analysis of the navigation law (3.10).

Proposition 3.1. Let L be a given number. Suppose that assumptions (3.4), (3.8), (3.9) and (3.12) hold. Then, the navigation law (3.10) is encircling.

Proof of Proposition 3.1. The trajectory of the robot with the navigation law (3.10) consists of three parts. In the first part, the robot moves along a minimal turning radius circle in the clockwise direction if $L + \dot{d}(0) < 0$ and in the counterclockwise direction if $L + \dot{d}(0) > 0$. It follows from (2.3b) and the assumption (3.8) that with this navigation law $\lambda_R(t)$ is increasing if $L + \dot{d}(0) < 0$ and $\lambda_R(t)$ is decreasing if $L + \dot{d}(0) > 0$. Switching to the second part of the trajectory occurs when $\dot{d}(t_*) = -L$ for some time t_*. It is obvious from Eqs. (2.3a) and (3.12) that $\lambda_R(t_*) = \arccos(\frac{L}{V_R})$. In the second part of trajectory, condition $\dot{d}(t) = -L$ holds and this part of trajectory is a sliding mode belonging to the surface $\lambda_R = \arccos(\frac{L}{V_R})$. Furthermore, it is obvious from the Eq. (3.10) that the vector field of the closed-loop system (2.3), (3.10) in a neighborhood of this sliding surface looks like the one shown in Fig. 2. Therefore, the trajectory of the system after switching to the second part of the trajectory remains at the surface $\cos(\lambda_R) = \frac{L}{V_{R0}}$. Second part of the trajectory is a so-called sliding mode (see e.g., ref. [44]). Since the target is steady, it follows from Eq. (2.3a) that

$$\dot{d}(t) = -V_{R0}\,\cos(\lambda_R(t))$$

https://doi.org/10.1017/S0263574709990294

for this part of the trajectory. Since $\dot{d}(t) = -L$, $d(t)$ is linearly decreasing over the second part of the trajectory. Therefore, switching to the third part of the trajectory occurs when $d(t)$ becomes so small that the constraint (3.7) does not allow to keep the angle λ_R constant anymore. This occurs when $\frac{V_{R0}}{d(t)} \sin \lambda_R = \omega_{\max}$. This and Eq. (3.5) imply that $d(t) = R_{\min} \sin \lambda_R$ at the time t of the switching. Now it follows from a simple geometry that the steady target lies inside the corresponding minimal radius circle, and the robot will move around the target along a minimum radius circle in the counterclockwise direction during the third part of the trajectory. This completes mathematical analysis of the proposed navigation law (3.10).

Remark 3.1. It follows from the mathematical analysis that during the most important part of the robot trajectory with the navigation law (3.10) corresponding to the sliding mode with the surface $\dot{d}(t) = -L$, the angle λ_R between the robot heading and the direction to target remains constant. That is why the navigation law presented in this paper is termed equiangular navigation guidance law. The geometry of motion with a constant angle between the heading and the direction to the steady target is described by the so-called equiangular spiral (see e.g., ref. [27]). Insects have been observed to follow such a spiral toward a candle or in a similar manner falcons toward their target (see e.g., refs. [42, 43]), hence, the ENG law can be viewed as biologically inspired.

Remark 3.2. In reality, due to limitations in switching frequency and delay, a switched controller will lead to chattering which is undesirable in practice. Chattering involves high control activity and may excite high-frequency dynamics neglected in modeling. In order to minimize or eliminate chattering, the control discontinuity is smoothed out in a thin boundary layer neighboring the switching surface with a linear interpolation of the sign function within the boundary layer. In this regards, the sgn is substituted with saturation function, shown in Fig. 3, in input control. The ENG law is then modified based on the argument above, as follows

$$\omega_R = \omega_{\max} sat\left(\frac{L + \dot{d}}{\varepsilon}\right), \tag{3.13}$$

where ε is the boundary layer thickness. The system robustness and smoothness of the control action are functions of boundary layer thickness. As $\varepsilon \to 0$, saturation function converges to the sgn function, the robustness of the system increases, however, it intensifies the discontinuity of the control action and chattering.[38] Note that in order to attenuate the effect of chattering in practice the more effective super twisting algorithm was proposed,[4,24] which will be studied in our future research.

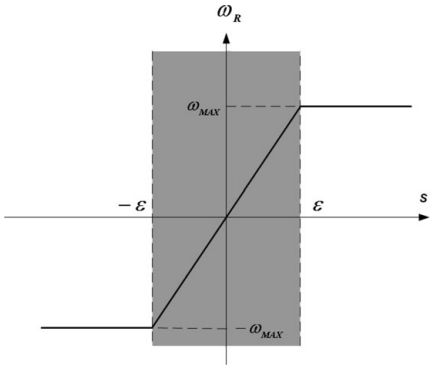

Fig. 3. Control interpolation in the boundary layer.

4. Obstacle-Avoidance Strategy

Navigation of a mobile robot toward a target in the presence of obstacles is more challenging and difficult. The robot has to operate in a real and unprepared environment without a priori information about the position of obstacles, their shapes, or their geometric distribution. The robot is assumed to be equipped with a set of range sensors, laser or sonar, situated equidistantly and counterclockwise on its perimeter. The sensors detect an obstacle in case it lies within the maximum range of view and provide its range and angle to the robot's moving direction. An algorithm is proposed to detour an enroute obstacle by maintaining a constant distance to the obstacle's boundary with following a smooth curve with the same center of curvature. The idea of this obstacle avoidance strategy originates from biology where it was called negotiating obstacles with constant curvature (see e.g., ref. [23]). An example of such a movement is a squirrel running around a tree or steering a vehicle around a bend in a road.

4.1. Reflection cone of range sensors

Consider Fig. 4 in which the robot encounters an enroute obstruction. The laser scanner transmits the signals in all directions in its field of view (FOV), which is assumed to be sufficiently wide.[7] The cone is generated by the reflected signals from the obstacle is termed reflection cone, which provides the necessary information (range and angle) about each point on the surface of the obstacle which is within the detectable area, shown as the shaded part in Fig. 4. In this figure, α is the maximum cone width of the reflection cone, which is fixed and depends on the number of range sensors and their physical dispositions. Furthermore, ϕ_1 and ϕ_2 are the angles of the boundary rays of the cone, i.e. the first and the last rays of reflection cone, with the robot's moving direction.

4.2. Avoidance command

An obstacle avoidance strategy is proposed with reference to Fig. 5. In the proposed strategy, the velocity vector of the

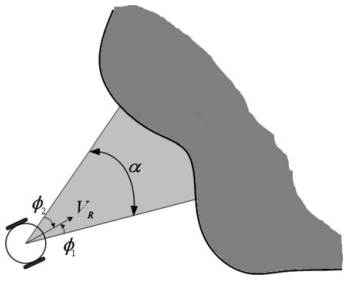

Fig. 4. Reflection cone of sensors.

https://doi.org/10.1017/S0263574709990294

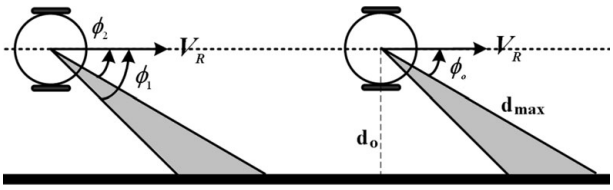

Fig. 5. Avoiding the obstacle while preserving a constant avoiding angle.

robot establishes a constant angle $\phi_o, 0 < \phi_o < \frac{\pi}{2}$, termed avoiding angle, outside the reflection cone with one of the two boundary rays which is nearer to the moving direction of the mobile robot. In other words, at each time, the robot pick a reference point on the obstacle surface and tries to modify its moving direction in order to establish a constant avoiding angle. In Fig. 5, since ϕ_2 is smaller than ϕ_1, the instantaneous velocity vector of the robot is modified so that $\phi_2(t) \to \phi_o$ as $t \to \infty$, which would result in the robot preserving a constant distance from the obstacle. Considering $\phi = \min(\phi_1, \phi_2)$, the commanded angular velocity of the robot in the proposed approach is defined as follows:

$$\omega_R = \omega_{\max} sgn(\psi), \tag{4.14}$$

where,

$$\psi = \begin{cases} \phi - \text{sgn}(\phi)\phi_o, & \text{if } V_R \text{ lies within the reflection cone} \\ \phi + \text{sgn}(\phi)\phi_o, & \text{if } V_R \text{ lies outside the reflection cone.} \end{cases} \tag{4.15}$$

Figure 6, shows four different cases under which the robot encounters an obstacle. ϕ_*^+ and ϕ_*^- denote the positive and negative angles, respectively. In Fig. 6(a), for example, the velocity vector of the robot is inside the reflection cone and $\phi = \phi_2^-$. Applying the proposed approach, we obtain $\psi = \phi + \phi_o$. In order for the robot to bypass the obstacle from the left and turn counterclockwise as the shorter path, we should have $\phi_o > |\phi|$ and as $|\phi| \leq \alpha/2$, it is assumed that $\phi_o > \alpha/2$.

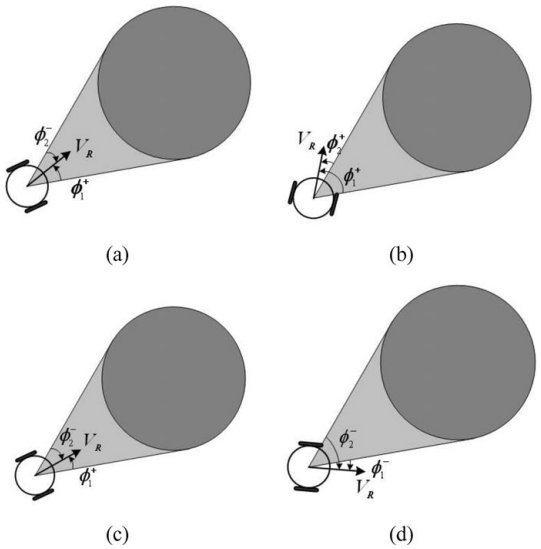

Fig. 6. Different cases of encountering an obstacle.

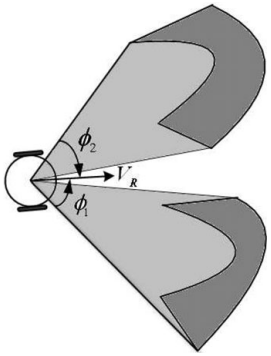

Fig. 7. Encountering two enroute obstacles.

As a result $\omega_R = \omega_{\max}$ and the robot turns to the left in order to enlarge the avoiding angle to ϕ_o and detour around the obstacle. Similar arguments can be contrived for other cases in order to derive the related avoidance commands. In the case of detection more than one obstacle on the way, as shown in Fig. 7, the angles of the first and the last emanated sensor rays in each scan with respect to velocity vector of the mobile robot are termed ϕ_1 and ϕ_2, respectively, and the avoidance strategy is applied. When $\phi_1 = \phi_2$ one direction is chosen by definition. If there is no reflection cone or if the velocity vector lies outside the cone while making an avoiding angle bigger than ϕ_o with the nearer boundary ray, the ENG law is sufficient to navigate the robot toward the target.

Remark 4.1. Having applied the proposed approach, a safety distance d_0 is preserved to obstacles which can be adjusted depending on the robot's physical characteristics as a function of $d_{\max}$ and ϕ_o.

We now present a mathematical justification of the navigation law (4.14) and (4.15).

Consider the case of a single obstacle. It is assumed that the obstacle's boundary is a smooth planar curve $B(x, y)$, where (x, y) are the coordinates in the plane. Furthermore, let $k(x, y)$ be the curvature of $B(x, y)$. Here we use the following standard definition of curvature (see e.g., ref. [36]). Let a plane curve $B(x, y)$ be given parametrically as $B(x(t), y(t))$ where $x(t)$, $y(t)$ are given smooth functions, then the curvature is

$$k(x, y) := \frac{x'y'' - y'x''}{(x'^2 + y'^2)^{3/2}}.$$

It should be pointed out that we do not assume that the curvature $k(x, y)$ is positive, for instance, in Fig. 8, the segment $(P_1P_2P_3)$ of the obstacle boundary has a positive curvature and the segment $(P_1P_4P_3)$ has the negative curvature. Furthermore, the curvature radius of the curve $B(x, y)$ is $R(x, y) := \frac{1}{|k(x,y)|}$.

Definition 4.1. A navigation law is said to be obstacle avoiding with the safety distance d_0 if the distance between the robot and the obstacle is not less than d_0 at any time.
Suppose that the following assumptions holds

$$\phi_o > \frac{\alpha}{2}, \tag{4.16}$$

https://doi.org/10.1017/S0263574709990294

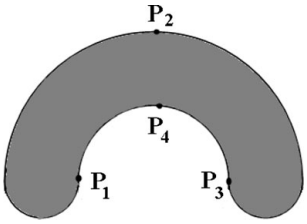

Fig. 8. A possible obstacle.

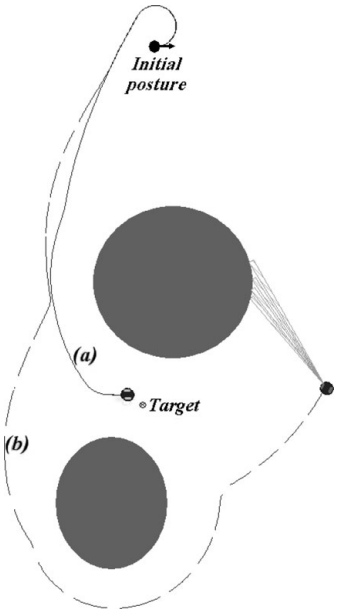

Fig. 9. Approaching a target with different values of $d_{\max}$.

$$R(x, y) > d_{\max} \quad \forall (x, y) \in B(x, y) : k(x, y) < 0. \quad (4.17)$$

Furthermore, Let

$$R_{\min} < \sqrt{R(x, y)^2 - d_{\max}^2 \cos^2 \phi_o} + \operatorname{sgn}(k(x, y)) d_{\max} \sin \phi_o \quad (4.18)$$

for all $(x, y) \in B(x, y)$. Now introduce the following constant

$$d_0 := \sup_{(x, y) \in B(x, y)} |\sqrt{R(x, y)^2 - d_{\max}^2 \cos^2 \phi_o} + \operatorname{sgn}(k(x, y)) d_{\max} \sin \phi_o - R(x, y)|. \quad (4.19)$$

Note that the parameter $d_{\max}$ should be large enough to warn the robot well in advance when the robot is on the collision course. On the other hand, selecting a too large value of $d_{\max}$ makes the cone unnecessarily large, more deviation from the ENG trajectory and probably loosing the targets in the vicinity of the obstacles. Robot trajectories in similar situations for two different values of $d_{\max}$ are shown in Fig. 9. The robot with a smaller $d_{\max}$, in trajectory (a), has the ability to reach the target; however, since the target is located between two obstacles, it is not accessible by the robot with a larger value of $d_{\max}$.

Suppose that assumptions (4.16), (4.17), and (4.18) hold and Let d_0 be a given number defined by (4.19). Then, we show that the navigation law (4.14) and (4.15) is obstacle avoiding with the safety distance d_0.

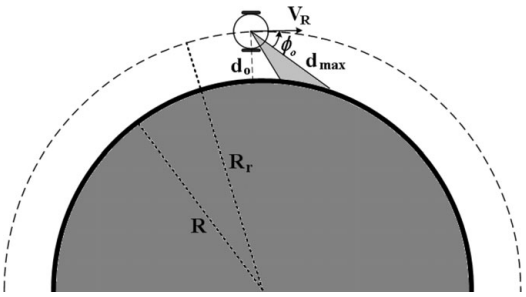

Fig. 10. Moving around a convex obstacle.

Indeed, according to the law (4.14), if $\psi(t) \neq 0$ the robot will move along a minimum radius circle until $\psi(t) = 0$. The parameter $d_{\max}$ should be large enough for the robot to achieve the condition $\psi = 0$ while keeping the distance from the obstacle greater than d_0. It is obvious that this condition is satisfied if

$$d_{\max} > 2R_{\min} + d_0. \quad (4.20)$$

In the reality, the condition (4.20) is too conservative and in simulations we take $d_{\max} := 2R_{\min}$. Furthermore, when the robot achieves the condition $\psi = 0$, it will move along a switching surface defined by this equation. Finally, the robot will move along a smooth curve around the obstacle. In a simplest cases, when a segment of the obstacle boundary is a circle of radius R, the robot will move along a circle with the radius

$$R_r = \sqrt{R^2 - d_{\max}^2 \cos^2 \phi_o} + d_{\max} \sin \phi_o$$

in the convex case (see Fig. 10) and along a circle with the radius

$$R_r = \sqrt{R^2 - d_{\max}^2 \cos^2 \phi_o} - d_{\max} \sin \phi_o$$

in the concave case (see Fig. 11). Hence, under the assumptions (4.18) and (4.20), the proposed navigation law (4.14) is obstacle avoiding with the safety distance d_0 where d_0 is defined by Eq. (4.19).

Remark 4.2. Notice that in the case where the obstacle curvature $k(x, y) \to 0$, hence, $R(x, y) \to \infty$ or, in other words, a segment of the obstacle boundary is close to a straight line, it follows from Eq. (4.19) that $d_0 \to d_{\max} \sin \phi_0$.

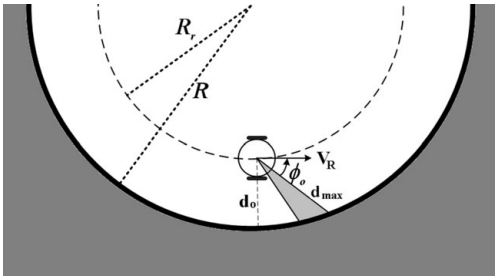

Fig. 11. Moving around a concave obstacle.

https://doi.org/10.1017/S0263574709990294

Indeed,

$$\sqrt{R(x,y)^2 - d_{\max}^2 \cos^2\phi_o} - R(x,y) = -\frac{d_{\max}^2 \cos^2\phi_o}{\sqrt{R(x,y)^2 - d_{\max}^2 \cos^2\phi_o} + R(x,y)}. \quad (4.21)$$

It is obvious that

$$-\frac{d_{\max}^2 \cos^2\phi_o}{\sqrt{R(x,y)^2 - d_{\max}^2 \cos^2\phi_o} + R(x,y)} \to 0,$$

as $R(x,y) \to \infty$. From this and (4.21), we have

$$\sqrt{R(x,y)^2 - d_{\max}^2 \cos^2\phi_o} - R(x,y) \to 0,$$

as $R(x,y) \to \infty$. This and Eq. (4.19) imply that $d_0 \to |sgn(k(x,y))d_{\max}\sin\phi_0| = d_{\max}\sin\phi_0$.

Remark 4.3. It should be pointed out that the proposed navigation strategy is based on sliding mode control. In our future research, we will apply more advanced sliding mode control algorithms such as integral sliding mode control.[6,12,45]

5. Navigation Algorithm

The basic navigation algorithm, shown in Table I, mixes the ENG law and the avoidance command in order to safely navigate the robot in an unknown environment. In the proposed algorithm, the robot has the ability to change the trajectory in real-time in order to detour an obstacle as soon as the obstacle appears on the way.

An explanation of the concept behind the proposed approach can be presented with reference to Fig. 12. Ignoring the presence of obstacle, in the nominal trajectory generated by the ENG law, trajectory (a), the robot travels through the obstacle while moving toward the stationary target along an equiangular spiral. Having applied the proposed idea, considering an obstacle on the way, the robot moves along the trajectory (b) and approaches the target. Several intermediate points have been shown on the trajectory. As while as there is no reflection cone, the robot moves along the same trajectory

Table I. Pseudo code for the navigation algorithm.

If	(There is a reflection cone)	Then
	$\phi = \min(\phi_1, \phi_2)$	
	If (V_R is inside the cone)	Then
	$\psi = \phi - \text{sgn}(\phi)\phi_o$	
	Else If $\phi < \phi_o$	Then
	$\psi = \phi + \text{sgn}(\phi)\phi_o$	
	Else $\psi = L + \dot{d}$	
	End	
Else	$\psi = L + \dot{d}$	
End		
	$\omega_R = \omega_{\max} sgn(\psi)$	

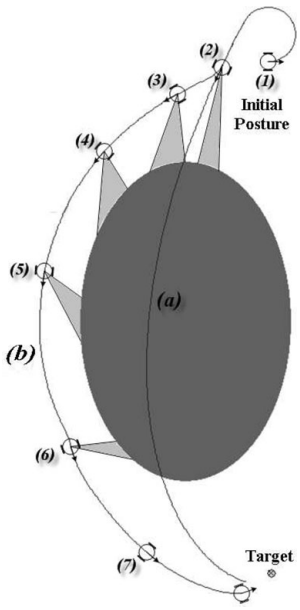

Fig. 12. Illustration of navigation approach.

as trajectory (a). At point (2), the range sensors detect an enroute obstacle. The velocity vector is outside the reflection cone; however, since the avoiding angle is less than ϕ_o, it turns clockwise in order to enlarge the avoiding angle and bypass the obstacle. Points 3, 4, and 5 show the robot detouring the obstacle with a constant avoiding angle and a safety distance. The velocity vector at point 6 is outside the cone and avoiding angle is larger than ϕ_o, hence, the navigation algorithm switches to the ENG and the robot approaches the target.

6. Computer Simulations

This section presents computer simulation results for a robot moving in an unprepared environment. Matlab and Mobotsim 1.0 simulator, which is a 2D easy to use graphical mobile robot simulator,[33] have been utilized for simulation purposes and testing. Simulation parameters have been shown in Table II.

Remark 6.1. The proposed navigation algorithm with a slight change is also applicable for guidance toward a maneuvering target. However, in this paper only stationary targets are considered and the simulation results for the case of maneuvering targets will be in a forthcoming paper.

The navigation algorithm is applied to various obstacle avoidance problems, and the results are shown. The only available information from the target is the LOS range, d.

Table II. Simulation parameters 1.

Parameter	Value	Comments
t_s	0.1 s	Sampling intervals
V_R	0.5 m/s	Robot linear velocity
$\omega_{\max}$	0.6 rad/s	Maximum angular velocity
ε	0.1	Boundary layer thickness
D_p	0.5 m	Robot platform diameter
$d_{\max}$	1.5 m	Sensor's maximum measurable range

https://doi.org/10.1017/S0263574709990294

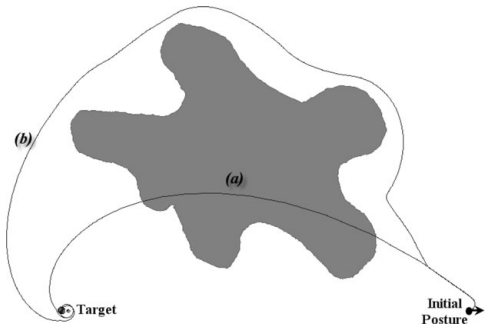

Fig. 13. Robot navigation toward a target (a) without obstacle, (b) in the presence of obstacle.

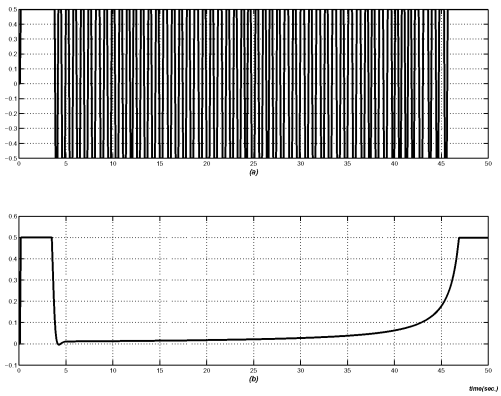

Fig. 14. ENG's commanded angular velocities, (a) using the sign function and (b) using the saturation function.

As shown in Fig. 13 trajectory (a), ignoring the presence of obstacle in the nominal trajectory generated by the ENG law with $L = 0.4$, the robot moves toward the target with constant linear velocity and a nearly constant approaching angle λ_R along a semi-equiangular spiral. The value of L is fixed throughout the experiment. A comparison of the ENG's commanded angular velocities using the sign and saturation functions has been shown in Fig. 14. Having applied the ENG using the sign function, the resulted angular velocity is a high-frequency signal, which as noted before leads to chattering. In order to minimize the chattering, the modified ENG proposed in Eq. (3.13) is applied. Since the boundary layer thickness is small, the robot trajectory is almost as the same as the trajectory (a) shown in Fig. 13. However, the derived angular velocity is smoother than that produced by the sign function. The range finders, equipped onboard, are able to detect the obstacles if they are within the detectable area. Trajectory (b) in Fig. 13 shows the robot encountering a stationary obstacle while safely navigate toward the goal. Note that, changing the referenced avoiding angle ϕ_o or the maximum radius of the cone $d_{\max}$, the safety distance between the robot and the target will change.

Figure 15 displays a U-shape obstacle in which some strategies, such as the potential field method, fail to find a solution and the problem of local minima happens.[21] Applying Eq. (3.13), since the ENG's spiral turning direction is counterclockwise, the robot has to turn around once to find a safe way toward the goal, shown in Fig. 15 trajectory (b).

Robot trajectory in confrontation with more challenging environment is shown in Fig. 16 in which the robot

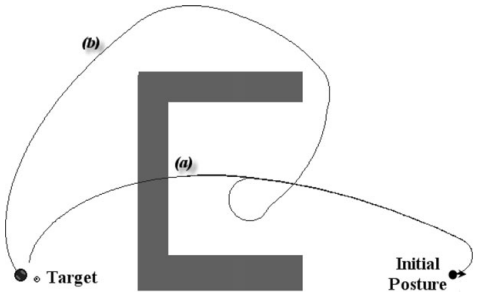

Fig. 15. Online robot navigation (a) without obstacle, (b) in the presence of a U-shape obstacle.

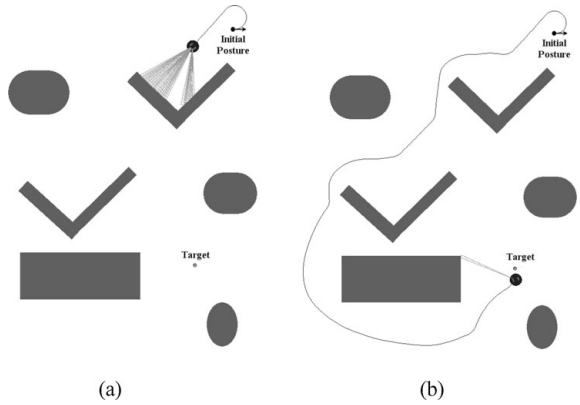

Fig. 16. Avoiding obstacles.

Fig. 17. Pioneer 3-DX robot which is equipped with Laser and Sonar range finders.

encounters corner situations on the way toward the target. Applying the navigation strategy, the robot successfully avoids the obstacles and approaches the target.

7. Experimental Results

To verify validity and study the performance of navigation approach in practice, various tests have been conducted on an ActivMedia Pioneer 3-DX robot. The robot is controlled using its onboard PC and is equipped with a Sick laser scanner, which gives the distance and angle to the obstacle if it is within the detectable area (see Fig. 17). To implement the navigation algorithm, we use C++ and active media robotics interface application (ARIA), which is an object oriented C++ library for controlling ActivMedia mobile robots,[1] running in the Linux operating system.

Remark 7.1. Throughout the experiments carried out in this paper, the odometry system has been used to obtain

https://doi.org/10.1017/S0263574709990294

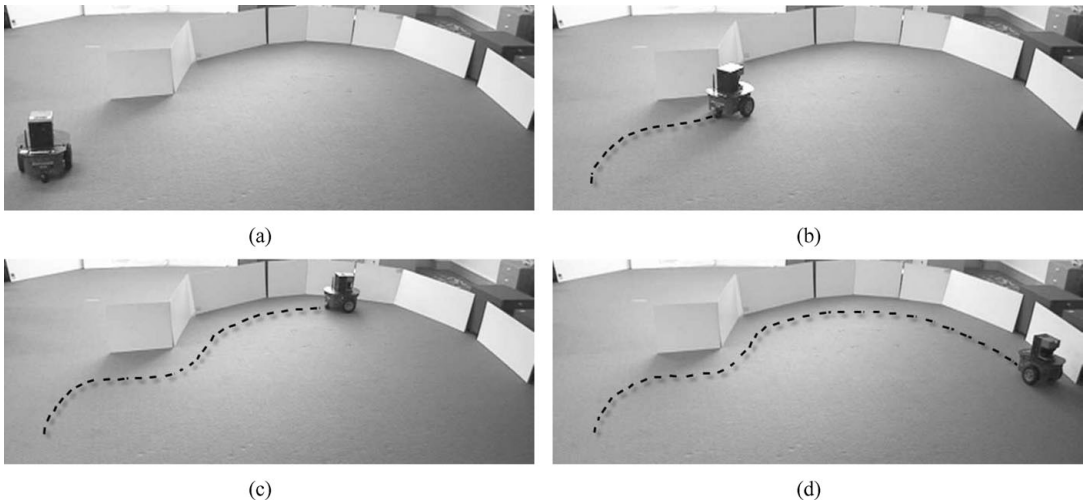

Fig. 18. Avoiding a U-shape obstacle in the first experiment.

the distance between the robot and target at each time. In doing so, the initial position of the robot is considered as the origin of a global coordinate system and the target position is predefined at (5 m, 0) for the first scenario, and (10 m, 0) for the second scenario. Hence, knowing the robot position at each time, using odometry information, the relative distance between the robot and target is calculated. It should be pointed out that during the experiments we do not use GPS.

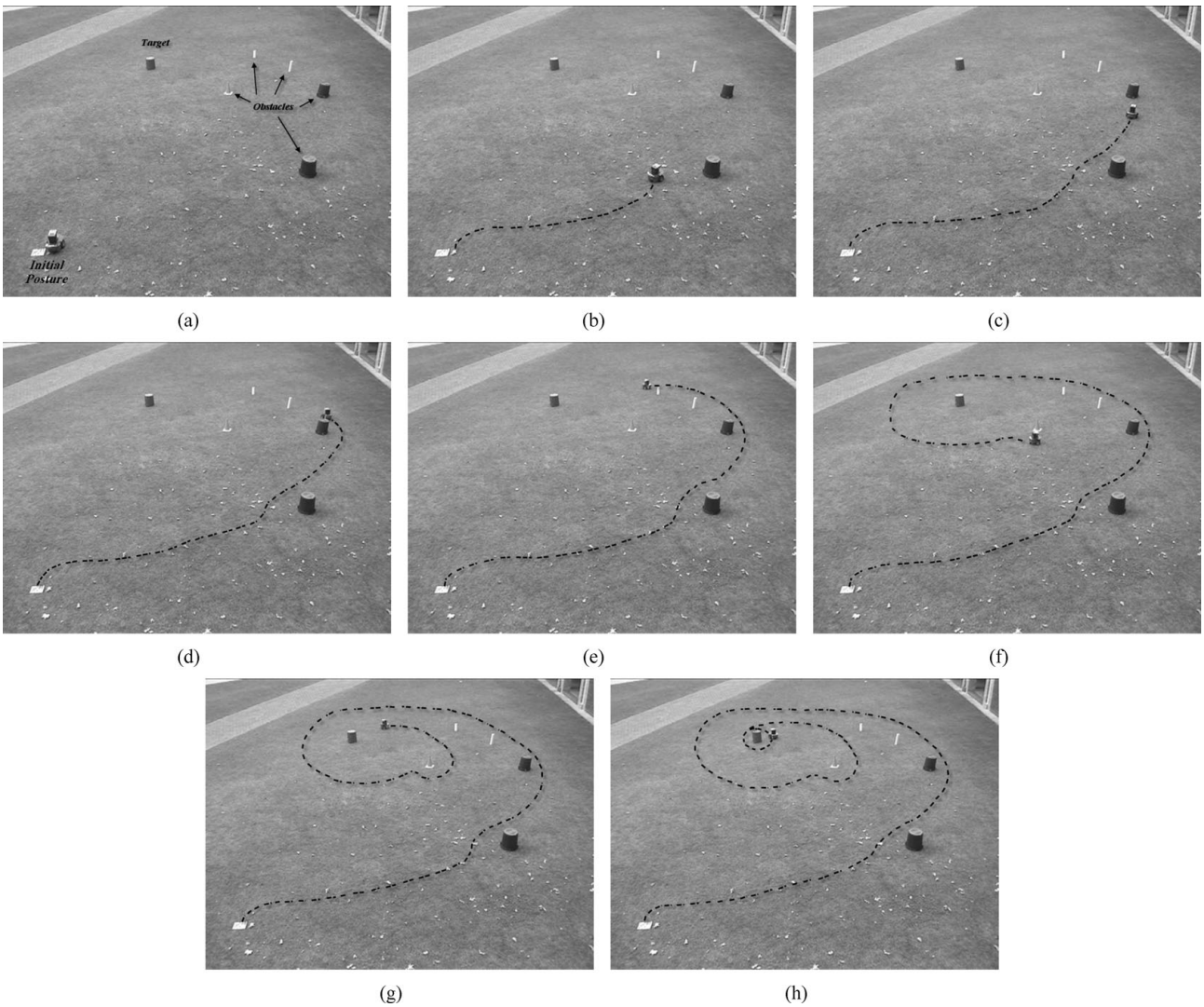

Fig. 19. Approaching a target in the presence of obstacles in the second experiment.

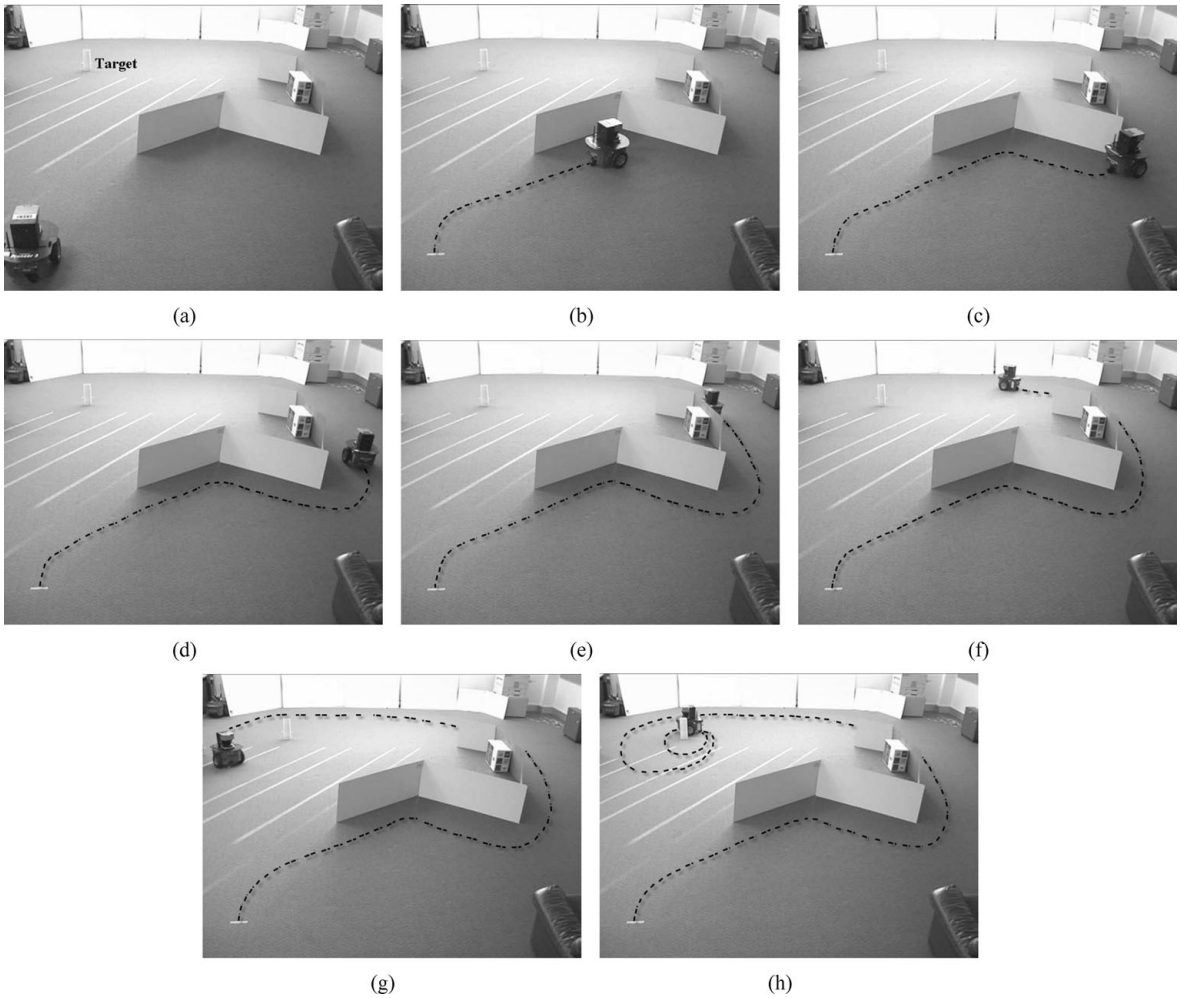

Fig. 20. Approaching a steady target in the presence of obstacles in the third experiment.

The experimental parameters set as $V_R = 0.4$ m/s, $\omega_{\max} = 0.7$ rad/s, $d_{\max} = 1.5$ m, $D_p = 0.5$ m, $L = 0.16$.

We consider an unknown environment. No information is available on obstacles positions and their geometric distributions. In order to show the performance of the proposed strategy in a real environment, three different experiments have been performed. Figure 18 shows four different snapshots of the first experiment which has been conducted indoor. The robot trajectory is depicted with dashed lines. This experiment illustrates how the robot behaves when it encounters an enroute U-shape obstruction. The target position is not shown in this figure.

The second experiment, shown in Fig. 19, is an outdoor scenario with a target position predefined at (10 m, 0). Several obstacles have been added to the nominal trajectory of the robot toward the target. Applying the proposed navigation strategy, the robot bypasses the obstacles while approaching the target with a constant linear velocity.

Figure 20 shows the third experiment which is another indoor scenario, at which the target position is predefined at (5 m, 0). In this experiment, the robot encounters a V-shape obstruction on its way toward the target. Eight different snapshots of this experiment are depicted in Fig. 20. The robot approaches the target while bypassing the obstruction with a predefined safety distance, and eventually goes into a circular trajectory around the target. In order to compare the simulation and experimental results, we perform another simulation (Fig. 21) with the same parameters and similar environment as the third experiment. As shown in Fig. 21(b), the robot trajectory toward the target in simulation

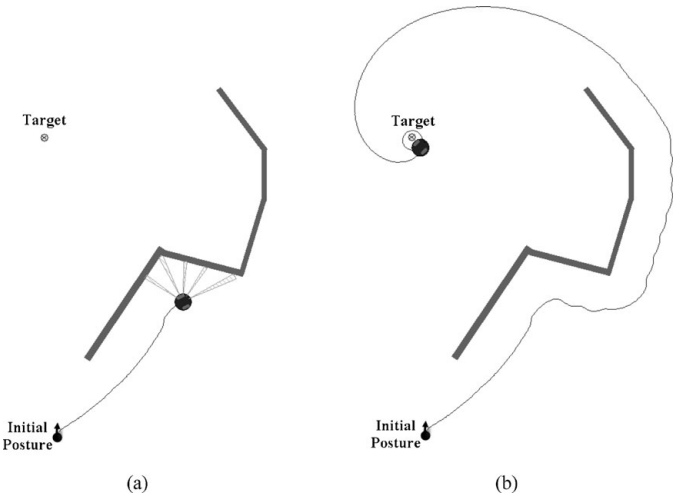

Fig. 21. The simulation result in a scenario which is similar with the third experiment.

https://doi.org/10.1017/S0263574709990294

is completely similar with the one obtained in the real experiment, depicted in Fig. 20(h).

8. Conclusion

The problem of safe navigation of a wheeled robot toward an unknown target in a cramped environment has been considered and a new biologically inspired navigation approach has been proposed. The algorithm alternates between two different modes: a goal-directed navigation which is the equiangular navigation guidance law, and a local obstacle avoidance technique. Using the sensory information, in avoidance mode, the reflection cone is used to maintain a fixed avoiding angle to the surface of the enroute obstacles. Having applied the proposed collision avoidance approach, the robot is able to avoid obstacles in real-time, while preserving a predefined safety margin. It was shown that the proposed navigation approach for reaching a target while skillfully avoiding the obstacles can be realized in a complex environment composed of multiple obstacles.

Acknowledgment

This work was supported by the Australian Research Council.

References

1. ActivMedia, "http://www.activmedia.com/."
2. F. Belkhouche and B. Belkhouche, "A method for robot navigation toward a moving goal with unknown maneuvers," *Robotica* **23**, 709–720 (Nov. 2005).
3. S. Belkhous, A. Azzouz, M. Saad, V. Nerguizian and C. Nerguizian, "A novel approach for mobile robot navigation with dynamic obstacles avoidance," *J. Intell. Robot. Syst.* **44**(3), 187–201 (Nov. 2005).
4. I. Boiko and L. Fridman, "Analysis of chattering in continuous sliding-mode controllers," *IEEE Trans. Autom. Control* **9**, 1442–1446 (2005).
5. V. Boquete, R. Garcia, R. Barea and M. Mazo, "Neural control of the movements of a wheelchair," *J. Intell. Robot. Syst.* **25**(3), 213–226 (1999).
6. F. Castanos and L. Fridman, "Analysis and design of integral sliding manifolds for systems with unmatched perturbations," *IEEE Trans. Autom. Control* **51**(5), 853–858 (2006).
7. P. Cerchie, B. Shipley, R. A. J. Wasson and D. Reago, "Manned simulation results concerning design parameters for an effective obstacle avoidance system (OASYS)," *J. Am. Helicopter Soc.* **37**(2), 3–10 (1992).
8. J. Chahl, M. Srinivasan and S. Zhang, "Landing strategies in honeybees and applications to uninhabited airborne vehicles," *Int. J. Robot. Res.* **23**(2), 101–110 (2004).
9. H. Choset, K. M. Lynch, S. Hutchinson, G. Kantor, W. Burgard, L. E. Kavraki, and S. Thrun, *Principles of Robot Motion: Theory, Algorithms and Implementations* (MIT Press, Englewood Cliffs, NJ, 2005).
10. B. d'Andrea Novel, G. Bastin and G. Campion, "Control of nonholonomic wheeled mobile robots by state feedback linearization," *Int. J. Robot. Res.* **14**(6), 543–559 (1995).
11. M. Deng, A. Inoue, Y. Shibata, K. Sekiguchi and N. Ueki, "An Obstacle Avoidance Method for two Wheeled Mobile Robot," *Proceedings of the 2007 IEEE International Conference on Networking, Sensing and Control*, London (2007) pp. 689–692.
12. S. Dong, "A comparison of sliding mode and integral sliding mode controls for robot manipulators," *Trans. Korean Inst. Electr. Eng.* **58**(1), 168–172 (2009).
13. J. Fasola, P. Rybski and M. Veloso, "Fast Goal Navigation with Obstacle Avoidance Using a Dynamic Local Visual Model Abstract," *Proceedings of SBAI'05, The VII Brazilian Symposium of Artificial Intelligence* (Sep. 2005) pp. 1–6.
14. R. Hartanto, F. Schonherr, M. Mock and J. Hertzberg, "Target-Oriented Mobile Robot Behaviors for Office Navigation Tasks," *Proceedings of the 2nd IEEE Workshop on Software Technologies for Future Embedded and Ubiquitous Systems (WSTFEUS 2004)*, Vol. 104–108 (May 2004) pp. 104–108.
15. Y. K. Hwang and N. Ahuja, "Gross motion planning: a survey," *ACM Comput. Surv.* **24**(3), 219–291 (Sep. 1992).
16. H. Ishiguro and N. Hagita, "Interactive humanoid robots for a science museum," *IEEE Intell. Syst.* **22**, (2007) pp. 25–32.
17. Z.-P. Jiang and H. Nijmeijer, "A recursive technique for tracking control of nonholonomic systems in chained form," *IEEE Trans. Autom. Control* **44**(2), 265–279 (1999).
18. I. Kamon, E. Rimon and E. Rivlin, "A range-sensor based navigation algorithm," *Int. J. of Robot. Res.* **17**(9), 934–953 (1991).
19. I. Kamon and E. Rivlin, "Sensory-based motion planning with global proofs," *IEEE Trans. Robot. Autom.* **13**(6), 814–822 (1997).
20. D. Katz and R. Some, "NASA advances robotic space exploration," *Computer* **36**(1), 52–61 (Jan. 2003).
21. Y. Koren and J. Borenstein, "Potential Field Methods and their Inherent Limitations for Mobile Robot Navigation," *IEEE International Conference on Robotics and Automation*, Sacramento (Apr. 1991) pp. 1398–1404.
22. L. Lapierre, R. Zapata and P. Lepinay, "Combined path-following and obstacle avoidance control of a wheeled robot," *Int. J. Robot. Res.* **26**(4), 361–375 (2007).
23. D. N. Lee, "Guiding movements by coupling taus," *Ecologic. Psychol.* **10**(3–4), 221–250 (1998).
24. A. Levant, "Sliding order and sliding accuracy in sliding-mode control," *Int. J. of Control* **58**, 1247–1263 (1993).
25. W. Lewinger, M. Watson and R. Quinn, "Obstacle Avoidance Behavior for a Biologically-Inspired Mobile Robot Using Binaural Ultrasonic Sensors," *IEEE/RSJ International Conference on Intelligent Robots and Systems* (Oct. 2006) pp. 5769–5774.
26. T.-H. S. Li, S.-J. Chang, and W. Tong, "Fuzzy target tracking control of autonomous mobile robots by using infrared sensors," *IEEE Trans. Fuzzy Syst.* **12**(4), 491–501, (Aug. 2004).
27. E. H. Lockwood, *A Book of Curves* (Cambridge University Press, Cambridge, 1961).
28. E. M. P. Low, I. R. Manchester and A. V. Savkin, "A biologically inspired method for for vision-based docking of wheeled mobile robots," *Robot. Auton. Syst.* **55**(10), 769–784 (2007).
29. V. Lumelsky and T. Skewis, "Incorporating range sensing in the robot navigation function," *IEEE Trans. Syst. Man Cybern.* **20**, 1058–1068 (1990).
30. V. Lumelsky and Stepanov, "Path-Planning Srategies for a Point Mobile Automaton Amidst Unknown Obstacles of Arbitrary Shape," **In**: *Auton. Robot. Vehicles* (I. J. Cox and G. T. Wilfong, eds.) (Springer, New York, 1990) pp. 1058–1068.
31. I. R. Manchester, A. V. Savkin and F. A. Faruqi, "Optical-Flow Based Precision Missile Guidance Inspired by Honeybee," *Proceedings of the 42nd IEEE Conference on Decision and Control*, Maui, Hawaii (Dec. 2003).
32. I. R. Manchester, A. V. Savkin and F. A. Faruqi–, "A method for optical-flow based precision missile guidance," *IEEE Trans. Aerosp. Electron. Syst.* **44**(3), 835–851 (2008).
33. M. R. S. Mobotsim 1.0, "http://www.mobotsoft.com/."
34. F. Mondada and E. Franzi, "Biologically Inspired Mobile Robot Control Algorithms," *NFP-PNR 23 Symposium*, Zurich, Switzerland (1993) pp. 47–60.
35. A. Ollero, A. Garcia-Cerezo and J. Martinez, "Fuzzy supervisory path tracking of mobile robots," *Control Eng. Pract.* **2**(2), 313–319 (1994).

36. A. V. Pogorelov, *Differential Geometry* (P. Noordhoff, Groningen, The Netherlands, 1959).
37. M. Quigley, B. Barber, S. Griffiths and M. Goodrich, "Towards Real-World Searching with Fixed-Wing Mini-UAVs," *Proceedings of IEEE/RSJ International Conference on Intelligent Robots and Systems*, Edmonton, Alberta, Canada (Aug. 2005) pp. 3028–3033.
38. S. H. Rya and J. H. Park, "Auto-tuning of sliding mode control parameters using fuzzy logic," *Am. Control Conf.* (Jun. 2001).
39. C. Samson and K. Ait-Abderrahim, "Feedback Control of a Nonholonomic Wheeled Cart in Cartesian Space," *IEEE International Conference on Robotics and Automation*, Sacramento, CA (1991) pp. 1136–1141.
40. S. Scheding, G. Dissanayake, E. Nebot and H. Durrant-Whyte, "Experiment in autonomous navigation of an underground mining vehicle," *IEEE Trans. Robot. Autom.* **15**(1), 85–95 (Feb. 1999).
41. H. Teimoori and A. V. Savkin, "A Method for Guidance of a Wheeled Mobile Robot Based on Received Radio Signal Strength Measurements," *Proceedings of the 17th IFAC World Congress*, Seoul, South Korea (Jul. 2008).
42. D. W. Thompson, *On Growth and Form* (Cambridge University Press, Cambridge 1966).
43. V. A. Tucker, "The deep fovea, sideways vision and spiral flight paths in raptors," *J. Exp. Biol.* **203**, 3745–3754 (2001).
44. V. I. Utkin, *Sliding Modes in Control Optimization* (Springer-Verlag, Berlin, 1992).
45. V. I. Utkin and J. Shi, "Integral Sliding Mode in Systems Operating Under Uncertainty Conditions," *Proceedings of the IEEE Conference on Decision and Control*, Kobe, Japan (1996) pp. 4591–4596.
46. N. Vlassis, N. Sgouros, G. Efthivolidis and G. Papakonstantinou, "Global path planning for autonomous qualitative navigation," *Conf. Tools with AI (ICTAI)* (Nov. 1996).
47. D. Voth, "A new generation of military robots," *IEEE Intell. Syst.***19**(4), 2–3 (Jul.–Aug. 2004).
48. R. Wegner and J. Anderson, "Agent-based support for balancing teleoperation and autonomy in urban search and rescue," *Int. J. Robot. Autom.* **21**(2), 120–128 (Apr. 2006).
49. J. M. Yang and J. H. Kim, "Sliding mode control for tracking of nonholonomic wheeled mobile robots," *IEEE Trans. Robot. Autom.* **15**(3), 578–587 (1999).
50. D. Yoon, S. Oh, G. Park and B. You, "A Biologically Inspired Homeostatic Motion Controller for Autonomous Mobile Robots," *Proceedings of the IEEE International consrrner on Robotics and Automation*, Taipei, Taiwan (Sep. 2003) pp. 3158–3163.